Detection of coherent terahertz radiation from a HTS Josephson junction by a semiconductor quantum dot detector

R. Shaikhaidarov, V.N. Antonov, and A. Casey
Physics Department, Royal Holloway University of London, Egham, Surrey TW20 0EX, UK

A Kalaboukhov and S. Kubatkin
MC2, Chalmers University of Technology, S-41296, Göteborg, Sweden

Y. Harada and K. Onomitsu
NTT Basic Research Laboratories, Wakamia, Atsugi-shi, Kanagawa-ken, 153-8902, Japan

A. Tzalenchuk
National Physical Laboratory, Hampton Road, Teddington, Middlesex TW11 0LW, UK and
Physics Department, Royal Holloway University of London, Egham, Surrey TW20 0EX, UK

A. Sobolev
Kotel'nikov Institute of Radio Engineering and Electronics RAS, 125009, Mokhovaya st. 11/7, Moscow, Russia
(Dated: January 27, 2016)

We examine the application of Josephson radiation emitters to spectral calibration of single-photon-resolving detectors. Josephson junctions were patterned in a YBCO film on a bi-crystal sapphire substrate and were voltage controlled to generate radiation in the frequency range of 0.05-1 THz. The detector used in this work consisted of a gate-defined quantum dot photon-to-charge transducer coupled to a single-electron transistor. Both the emitter and the detector were equipped with matching on-chip wide band antenna. The combination of a tuneable emitter and detector allowed us to determine the efficacy of the YBCO emitter and also to analyse the elementary processes involved in the detection.

PACS numbers: 74.50.+r,73.21.-b, 87.50.U-

I. INTRODUCTION

Cryogenic detectors of terahertz radiation with single photon sensitivity have been demonstrated in recent years [1–5]. Spectral calibrations of these detectors have been carried out using external terahertz sources, narrow-band filtered thermal sources or sources based on cyclotron emission from 2DEGs in strong magnetic field. None of these solutions are suitable when recurring calibrations in a wide range of frequencies are required to establish how the spectral characteristics of the detector have changed with time, but the payload is constrained in certain situations such as on a satellite. Here we examine a calibration solution based on a Josephson junction.

Voltage applied across a Josephson junction (JJ) causes oscillations of the dissipative current, and, correspondingly, the generation of electromagnetic radiation, with a frequency $f = 2eV_{JJ}/h$. The upper limit of the frequency is determined by the value of the superconducting gap. In S-I-S junctions the gap is related to the critical current and the normal resistance of the JJ, I_C and R_N, via the Ambegaokar-Baratoff relation, $I_C R_N = (\pi/2e)\Delta_S \tanh(\Delta_S/2k_BT)$, which for $T \to 0$ becomes $I_C R_N = (\pi/2e)\Delta_S$. In high temperature superconductors (HTS) Δ_S can be as large as 15 meV, which corresponds to $f \sim$7 THz. However, when the junction is shunted intrinsically, which is the case for HTS JJ, or extrinsically (by an external resistor) the radiation is suppressed below the gap value and is determined by $I_C R_N < \Delta_S/e$. Radiation emitted by HTS JJs has been the subject of intense research in recent years, motivated by the need for a spectral source of terahertz radiation. Individual JJs coupled to planar antennae are the simplest realisation of such terahertz sources, and they can deliver a narrow radiation line [6] with continuous tuning of frequency over a wide range. The overall power dissipated by the individual HTS JJ is $I_C V_{JJ}$, with the maximum V_{JJ} limited by $\sim I_C R_N$. Part of this power is dissipated as Joule heating, and only a fraction, typically few pW, is converted into coherent radiation [7, 8]. In a planar HTS JJ most of the coherent radiation remains inside the substrate, and only a small part is radiated into the environment because of mismatch of the dielectric constants between the substrate material and air/lens, and low coupling efficiency of the radiation of an individual JJ to the planar antenna. It is a formidable task to develop an accurate model of such a source of coherent radiation. An experimental assessment is also difficult because the coherent radiation is weak, and obscured by the strong blackbody radiation of the heated JJ. One needs a spectrally sensitive detector which would be blind to the blackbody radiation in order to succeed. The purpose of this paper is to show that the weak radiation of individual JJs can be detected, and it can be useful in the spectral calibration of the cryogenic detectors.

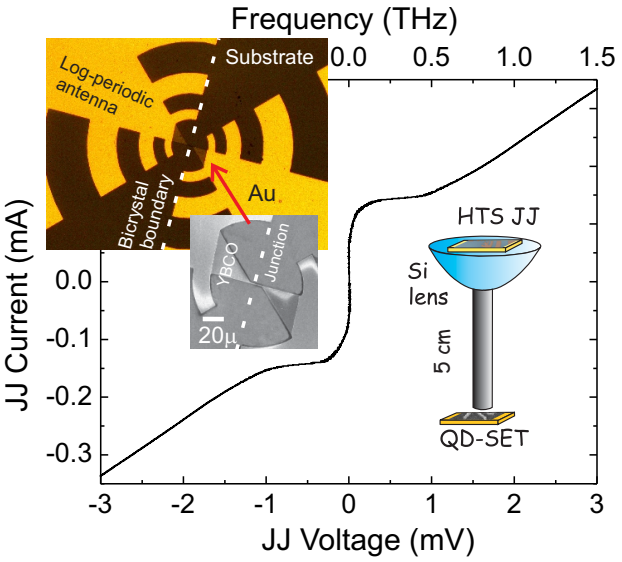

FIG. 1. $I-V$ curve of a HTS JJ taken at 0.02 K. Top axis is the Josephson frequency corresponding to the voltage across the JJ. Insets: optical image of a 2 μm wide HTS JJ defined at the bi-crystal boundary, and the optical scheme of the experiment.

It was recognised very soon after the discovery of the Josephson effect in 1962, that Josephson junctions can be used as a source of controllable coherent electromagnetic radiation at cryogenic temperatures. The first direct measurements of the emitted radiation were made by Yanson et al. in 1965 [9]. The radiation power, $W \sim 10^{-14}$ W, was estimated in these early measurements on low-T_c superconductors. This low power was attributed to a mismatch between the junction impedance and the impedance of the vacuum. There have only been a few attempts to measure the coherent radiation emitted by a HTS JJ. A hot electron bolometer and a separate HTS JJ have been used as detectors [10–12]. In these experiments the power of coherent radiation incident on a 0.5x0.5 mm^2 area of a bolometer was estimated to be $P_{osc} \sim 10^{-13}$ W, when the source and sensor were placed back to back [10]. This result however has a high level of uncertainty because of an inherent problem with Joule heating affecting detectors and variability related to the samples. Further study of individual planar HTS JJ has stalled as attention has recently focused on the properties of stacks of patterned intrinsic Josephson junctions in $Bi_2Sr_2CaCu_2O_8$. Emission of coherent radiation of up to 30 μW with a full width at half maximum (FWHM) as small as ∼50 MHz was reported [13–15]. The FWHM and central frequency in these devices are determined by the spatial resonance in the coupled JJs of the patterned stack. While demonstrating high power and a narrow line of emitted radiation these devices have one substantial drawback: their limited frequency tuning, less than 10%, which is achieved by varying the operation temperature.

In this work we return to the operation of an individual JJ. While inferior to stacked Josephson junctions in terms of the output power, they have an advantage in their ability to continuously tune the output frequency over a wide range. The HTS JJ in our device is coupled to a planar metallic logarithmic periodic antenna with a designed bandwidth of 0.2-2 THz. When a bias voltage is applied across the JJ it generates radiation in a frequency range up to 1 THz. The JJ radiation is probed by a quantum dot detector which has a single photon sensitivity, enabling spectroscopy of extremely low power coherent radiation. We observe two resonances in the photoresponse, at ∼0.3 THz and ∼0.8 THz, which can be attributed to an excitation of the resonance plasma oscillations in the detector. The resonances are relatively wide,∼30%, which is usual for the plasma excitations in a semiconductor material. It exceeds the FWHM of the coherent radiation of HTS JJ, which typically is ∼ 1 GHz for individual JJs [11]. We found that only a tiny part, 4×10^{-10}, of the power dissipated in the HTS JJ is emitted as coherent radiation into the vacuum. No particular resonances related to the planar antennae, or the shape of the HTS JJ, were seen.

II. EXPERIMENTAL RESULTS AND DISCUSSION

The experiments were carried out using two different measurement setups. The HTS JJs and QD detectors in both experiments were identical. In the first setup the HTS JJ and the QD detector were at 0.02 K of the mixing chamber of a dilution refrigerator. The HTS JJ is fixed on a semi-spherical Si lens coupled to a 5 cm light pipe, a stainless steel tube of 3 mm diameter, extended to the QD detector, see the inset in Fig. 1. The attenuation of the optical system was estimated to be 22 dB if we assume the quantum efficiency of the detector to be about 0.003 [16]. In our estimation we took the impedance of the QD and the antenna to be 300 Ω and 10 Ω at 0.3 THz respectively. In the second experimental setup a similar HTS JJ was fixed at the 4 K stage of a cryogen-free refrigerator in close proximity to the QD detector. Radiation emitted by the HTS JJ was delivered to the detector via the light pipe described above. A black polyethylene filter was used to filter out the infrared radiation. The QD detector is fixed in a metal enclosure at the 0.5 K stage.

A. HTS Josephson Junctions emitter

A grain boundary junction, integrated with a logarithmic periodic antenna was patterned by photolithography into a 200 nm thick YBCO film. The YBCO was grown by pulsed laser deposition on a sapphire bi-crystal substrate with the mis-orientation angle of 24° [17]. The junction has a width of 2 μm, and the antenna had an

outer diameter of 0.5 mm, see inset in Fig. 1. A typical current voltage ($I-V$) characteristic of HTS JJ is shown in Fig. 1. The shape of the $I-V$ curve indicates that the JJ is overdamped. There are no obvious resonances on the $I-V$ curve related to the coupling of the JJ to the metallic planar antennae. The $I_C R_N$ product of a typical JJ is ∼3.8 mV, and therefore a coherent radiation of up to ∼2 THz can be generated when 4 mV is applied. Only a small part of the dissipated power is however converted to coherent radiation at the Josephson frequency, while the largest part is dissipated via phonons and black body radiation. The latter becomes especially critical when the voltage across the JJ exceeds ∼1 mV, as the HTS JJ micro-bridge is then strongly overheated. The effective temperature of the microbridge, T_m, can be estimated using a simplified model $T_m = \sqrt{T_b^2 + 3(eV_{JJ}/2\pi k_B)^2}$, where T_b is the bath temperature [18]. For a V_{JJ} bias of ∼1 mV the effective temperature T_m can be as high as ∼3 K while the bath temperature T_b is only 0.26 K [9]. Overheating results in an increase in the black body radiation emitted by the HTS JJ. Because T_m grows linearly with V_{JJ} the incoherent black body radiation dominates over the coherent radiation at high bias voltages. In order to separate the two components of the radiation one needs a spectrally sensitive detector, which would detect only the coherent part of radiation. In Ref.[12] a separate individually tuned HTS JJ detector was used for such an experiment. However the analysis was inconclusive, because of the presence of a bolometric response of the detector to blackbody radiation. We utilise the QD detector which is robust against blackbody radiation when operating in the regime of excitation of plasma resonance in the QD.

B. Quantum Dot detector

The detector is a semiconductor QD coupled to an aluminium, single-electron transistor (SET). The QD is positioned at the focal point of a log-periodic antenna. The QD of a diameter D ∼1.4 μm is defined by a mesa pattern and a biased metal gate, see inset in Fig. 2. The two-dimensional electron gas (2DEG) has the electron concentration of $n_s \sim 1.45\text{x}10^{11}$ cm^{-2} and the mobility μ ∼1.2x10^5 cm^2/Vs at T=4 K. The QD has a few thousands electrons, and it can be considered to be a semi-classical object, in which plasma oscillations can be excited. These oscillations provide an efficient way of coupling terahertz radiation to the electron system in a semiconductor. From the mobility of the electron gas we can estimate the damping factor of the plasma oscillations, $1/(2\pi)f\tau_e$, which is smaller than 0.15 at f =0.25 THz, where τ_e is an electron scattering time. Therefore we can expect excitation of the plasma mode in the QD upon absorption of terahertz photons. The fundamental mode of plasma oscillations in the dot is determined by its diameter D and the carrier concentration n_s, $f^2 = e^2 n_s/\pi^2 \varepsilon_{eff} m^* D$, where ε_{eff} ∼7 is the effective dielectric constant at the vacuum/GaAs interface. For our device the formula gives the resonance frequency of f ∼0.23 THz. Plasma resonances in a QD of a slightly different size and design have been seen before [19]. In a QD of D ∼0.5 μm and $n_s = 0.9 \times 10^{11}$ cm^{-2} the resonance was at f ∼0.5 THz with the FWHM/f ratio of ∼30%. However estimation of the resonance frequency from the formula gave a smaller value, about 70% of that measured, which can be attributed to an uncertainty in the determination of the QD size. The FWHM decreases substantially, down to 5%, when a moderate magnetic field of 1 T is applied. The magneto-plasma resonance is then excited [20]. The QD is not sensitive to radiation with frequencies away from the resonance. The Drude absorption by the QD, the other photon absorption mechanism, is much weaker because of a large mismatch of the radiation wavelength and the size of the dipole related to individual electrons. Consequently the blackbody radiation of the overheated JJ, which would peak at ∼ 50 GHz, has a small effect on the operation of the QD detector. This is confirmed in the experiment where we observe the decrease of the photo-response at high bias V_{JJ}, where $f = 2eV_{JJ}/h$ exceeds the plasma resonance in the QD, while the black body radiation power is on rise.

The large FWHM of the plasma resonance implies that the lifetime of the excitation in the QD at zero magnetic field is short, only a few picoseconds. The plasma oscillations decay in a way that either charge polarisation is induced in the QD, or even charge is excited out of the QD. Polarisation of the charge density in the 2DEG is used in plasmonic detectors [4, 21–23]. In our experiment we consider the second mechanism – charge excitation of the QD. The detector is designed in such way that charge excitations of the QD are probed by a sensitive electrometer, SET. Details of the fabrication and the operation of the SET can be found elsewhere [24, 25]. Coulomb Blockade Oscillations (CBO) of the SET current are shown in Fig. 2. The period of the oscillations changes from 62.7 mV to 5.28 mV when the QD is formed at V_G ∼-0.654 V. The pattern of CBO is shifted by $\delta V_G = C_{SET}^{QD}/(C_\Sigma^{QD} + C_{SET}^{QD})\delta V_G^{Period}$ every time an electron leaves the QD because of the capacitive coupling C_{SET}^{QD} between the SET and the QD, where C_Σ^{QD} is the total capacitance of QD and δV_G^{Period} is the CBO period. For the present device the shift is ∼20% of δV_G^{Period} [24]. When the gate voltage V_G is fixed then the electron excitations are seen as step-like changes of the SET current, see Fig. 5(a). One can find the rate and the lifetime of the QD excitations by counting the number of SET current spikes and measuring the time spent in the excited state. The spikes are more frequent close to the gate voltage where the QD is just formed, V_G ∼ -0.654V, due to excitation of thermal electrons. These excitations were suppressed at more negative V_G when a

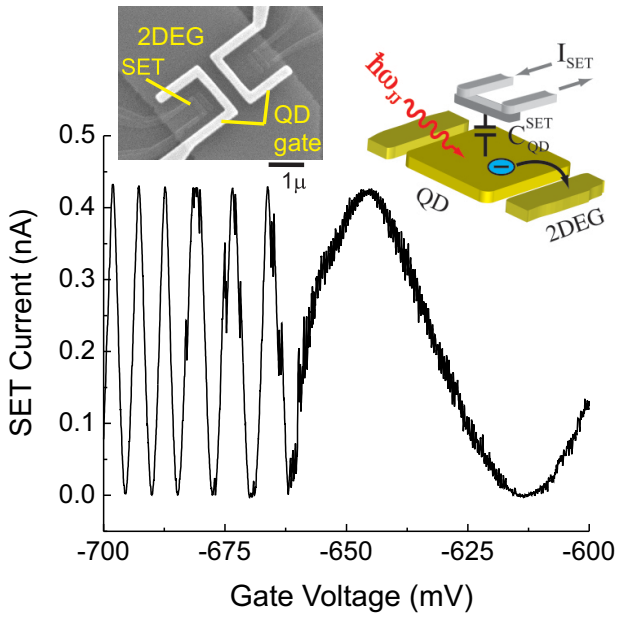

FIG. 2. CBO of the aluminium SET as a function of voltage on the QD gate. The CBO period changes at $V_G \sim$ -0.654 V when the QD is formed in the 2DEG. Inset: an SEM picture and operation scheme of the detector. The QD is formed in the 2DEG by the negatively biased QD gate and the edge of the mesa strip. The QD is capacitively coupled to the aluminium SET fabricated on top of the mesa strip. The SET current is sensitive to the excitation of electrons out of the QD upon absorption of THz photons.

high enough potential barrier was imposed by the gate voltage, see Fig. 3. Close to the pinch-off voltage the count rate can be modelled by an exponential decay of the form, $P = P_0 \exp(-a(V_G - V_{G0})/k_BT)$, with V_{G0} =-0.654 V being the threshold voltage where the QD is formed. The change in the electro-chemical potential of electrons and the applied gate voltage are related to each other by $\delta\mu = a\delta V_G$, where a=13.8 meV/V. We use the value of a later in the analysis. It is assumed that the tunnelling of electrons under the barrier is negligible because of the large width of the gate electrode. Then the charge excitations from the QD should take place only when the electron energy exceeds the potential barrier, for example in the case of absorption of a photon by the QD. Therefore the most sensitive operation of the detector is expected below -0.654 V. The SET current and the count rate coherently oscillate as seen in Fig. 3. The effect is a consequence of the Coulomb blockade of the electron excitations from the QD itself.

C. Detection of HTS JJ radiation

We measure the count rate with a fixed V_G, while changing the voltage across the HTS JJ. The results are shown in Fig. 4. There are two clear peaks with FWHM of 30% and the central frequencies close to $f \sim$0.3 THz and $f \sim$0.8 THz. The counting rate drops rapidly at frequencies above 0.9 THz and below 0.1 THz. It is important to note that the count rate drops at large bias voltages V_{JJ}, where incoherent black body radiation of the overheated HTS JJ should contribute to the photo-response. This contribution was seen in the experiment of Ref. [10], where a bolometer was used. The photo-response increased there as the square of the bias voltage, V_{JJ}^2, because the bolometer absorbs black body radiation emitted by the overheated JJ. We do not observe this effect, which clearly indicates that our detector does not respond to black body radiation, but rather detects coherent radiation at frequency f. The photo-response is seen however only in a narrow range of gate voltages V_G, from -0.654 V to -0.657 V. By using these voltages we can estimate the change of the effective potential in the vicinity of the 2DEG and consequently the increase of the barrier height confining electrons on the QD, $\delta U = a\delta V_G$ $\sim$40 μeV. This change is much smaller than the energy of the terahertz photons, $\sim$1 meV for f=0.3 THz. One would expect that photo-excitations should extend deep into negative V_G, which is not seen in the experiment. The effect can hardly be ascribed to a substantial change of the coupling of radiation to the QD. Probably it is a consequence of the suppression of the relaxation mechanism at low temperatures. If the tunnelling of electrons from the 2DEG electrodes into the QD is suppressed, then the QD can be multiply excited by absorbing consecutive photons. For a multi-excited QD the energy of a THz photon may not be enough to overcome the potential barrier forming the QD. We can estimate the order of excitation needed for such a situation by invoking the charging energy of the QD, $\sim$80 μeV [24]. Excitation of each electron out of the QD decreases the potential of the electrons in the QD by 80 μeV, so that the excitation of a dozen electrons should completely block further excitation. The energy of the absorbed photons can then be released by non-radiative phonon emission.

The frequency of the first resonance varies with the V_G from $\sim$0.18 THz at V_G=-0.6543 V to $\sim$0.4 THz at V_G=-0.6568 V. We estimate that the plasma resonance frequency in our device should be $\sim$0.23 THz. Since the resonance frequency varies as the square root of the size, the diameter of the QD should change by a factor of four in order to account for the observed frequency change. Such a dramatic effect can be explained only by the assumption that at small negative V_G the QD is not well defined, and the potential barriers are shallow, such that plasma waves of long wavelength can be excited. As V_G becomes more negative, the potential barrier becomes steeper, and the resonance appears to be better defined by the geometrical dimensions. The opposite trend is demonstrated by the resonance peak at high frequency. It moves towards the lower frequencies, from $\sim$0.85 THz at V_G=-0.6543 V to $\sim$0.7 THz at V_G=-0.6558 V, and then disappears, see Fig. 4.

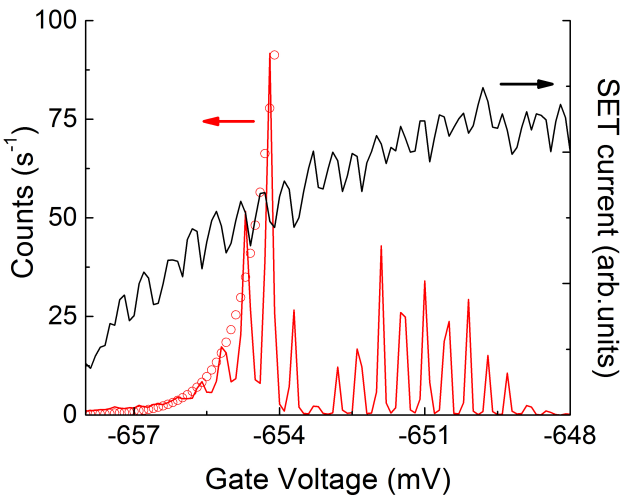

FIG. 3. Count rate of charge excitation of the QD due to thermal photons at T=0.02 K. Oscillations of the count rate are correlated with CBO of the QD seen in the SET current. Counts are suppressed below V_G ∼-0.657 V when QD is completely decoupled from the surrounding 2DEG. Open circles are the exponential fit of the suppression

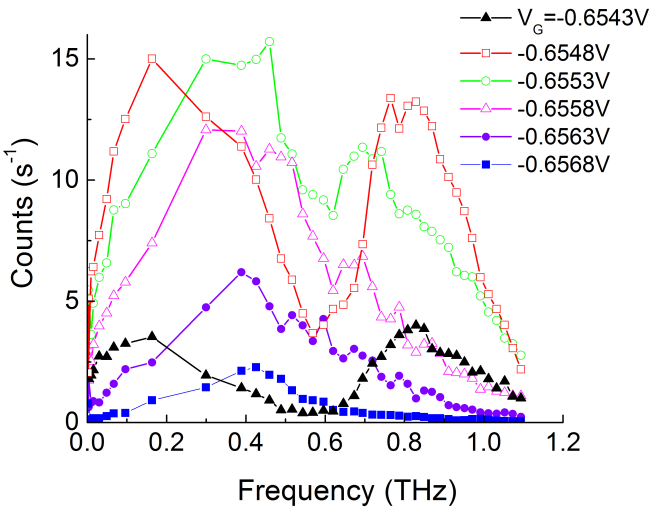

FIG. 4. Count rate of the QD detector under radiation emitted by a HTS JJ at different V_G . There are two peaks in the count rate, one close to 0.3 THz and the other around 0.8 THz.

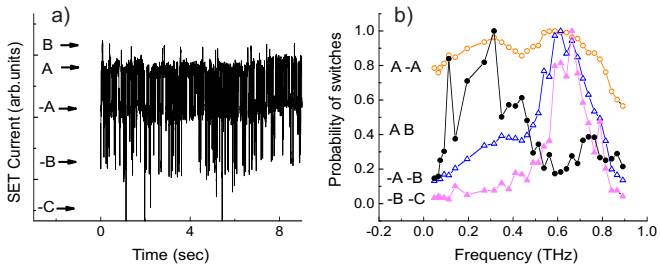

FIG. 5. (a) Time traces of SET current at 0.8 THz. There are few levels corresponding to different QD states: ground A and -A, excited B and -B, double excited -C (b) switches between different states normalized to maximum counts: AB switches has a maximum at 0.3 THz, -A-B and -B-C has a maximum at 0.7 THz, A-A has both resonances.

One can get further insight into the resonances from a more accurate analysis of the switching time traces, see Fig. 5, which allows deconvolution of various (de-) excitation processes of the QD. When the voltage across the HTS JJ corresponds, for example, to 0.8 THz, one can identify five states of the QD from Fig. 5(a): ground states A and -A (rigorous identification of the true ground state is impossible because these two states appear nearly as frequently in the time traces), first excited states B and -B corresponding to the excitation of one electron out/onto the QD, and the second excited state, -C, corresponding to the excitation onto the QD. The neighbouring states differ by one electron on the QD. We repeat this procedure for various V_{JJ}. The count rates in Fig. 4 are a sum of all excitations: -AA, -A-B, -B-C and AB, while in Fig. 5(b) we count each type of excitation separately. The A-A excitation has two peaks at 0.3 THz and 0.7 THz on a background of a high rate of dark switches. The -A-B and -B-C excitations have a dominant resonance peak at 0.7 THz, while the AB excitations have a peak at 0.3 THz. The sign of the SET current switches indicates that electrons are predominantly excited out of the QD at the 0.3 THz resonance, and they are excited into the QD at 0.8 THz. There are two possible origins of the 0.8 THz peak: a high order plasma mode in the QD, or the resonance plasma waves developed outside of the QD. The latter can be a plasma wave developed in the 2DEG between two QD gates, see the left insert in Fig. 2. The distance between the gates is 0.2 μm, which would give f ∼0.6 THz for the central frequency. The fact that electrons are excited to the QD at this resonance supports the explanation.

From our experiment we can estimate the ratio between coherent radiation and the total dissipated power of the HTS JJ. A typical increase of counting rate at the resonance compared to the background is ∼10 s^{-1}. The power of the coherent radiation detected by the QD-SET detector would be 2×10^{-21} J for $f \sim 0.3$ THz. If the attenuation of the optical system is 22 dB then the power emitted by the HTS JJ to the Si lens is 30 aW. The HTS JJ dissipates a total power of ∼80 nW, thus only 4×10^{-10} part is emitted as coherent radiation to the Si lens. A few factors can be considered in order to account for such a small value. A large part of the radiation is emitted along the surface of the substrate and does not enter the Si lens at all. Up to a quarter of the radiation stays in JJ itself, and a few percent is emitted into the vacuum opposite to the Si lens. Also we can not accurately account for the polarisation of the emitted radiation with respect to the detector when we estimate the quantum efficiency.

III. SUMMARY

We studied radiation emitted by HTS JJ using a QD detector. The QD detector allows us to probe the coherent part of the radiation. Two resonances are seen in the photo-response when we sweep voltage across the JJ, at ∼0.3 THz and ∼0.8 THz. We argue that the lower resonance is related to excitation of plasma waves in the QD of detector, while the origin of the second resonance is not exactly clear. Coherent radiation is only 4×10^{-10} part of the total power dissipated by the JJ. We believe that the small conversion factor is partially related to the weak coupling of HTS JJ to the planar antennae, a difference in the dielectric constant of the HTS JJ substrate and vacuum/lens material, and a possible polarisation mismatch. Although the individual HTS JJ coupled to a radiating antenna has an extremely low conversion efficiency of power to the coherent radiation, the emitters based on these devices can be useful for spectral calibration of cryogenic single-photon detectors, especially where recurring system self-calibration is required, and no other means would do, such as on a satellite. In addition they may also be useful as generators of coherent photons in application to cryogenic quantum simulators and computers. In applications where higher power is required alongside the wide-range tunability of individual JJ, phase-locked parallel-biased series arrays of HTS JJ may be employed [26, 27] (also see [28] for a review of JJ array radiation sources).

IV. ACKNOWLEDGMENTS

The work was supported by EPSRC grant EP/K016822/1

[1] S. Komiyama, O. Astafiev, V. Antonov, T. Kutsuwa, and H. Hirai, A single-photon detector in the far-infrared range, Nature, **403**, 40507 (2000)

[2] H. Hashiba, V. Antonov, L. Kulik, A. Ya. Tzalenchuk, P. Kleinschmid, S. Giblin, and S. Komiyama, Isolated quantum dot in application to terahertz photon counting, Phys. Rev. B **73**, 081310(R) (2006)

[3] P. Kleinschmidt, S. Giblin, A. Ya. Tzalenchuk, H. Hashiba, V. Antonov, and S. Komiyama, Sensitive detector for a passive terahertz imager, J. Appl. Phys. **99**, 114504 (2006)

[4] S. Pelling, R. Davis, L. Kulik, A. Tzalenchuk, S. Kubatkin, T. Ueda, S. Komiyama, and V. N. Antonov, Point contact readout for a quantum dot terahertz sensor, Appl. Phys. Lett. **93**, 073501 (2008)

[5] H. Hashiba, V. Antonov, L. Kulik, A. Tzalenchuk and S. Komiyama, Sensing individual terahertz photons, Nanotechnology **21**, 165203 (2010)

[6] Y.Y. Divin, J. Mygind, N.F. Pedersen, P. Chaudhari, Linewidth of Josephson oscillations in $YBa_2Cu_3O_{7-x}$ grain-boundary junctions, IEEE Trans. Appl. Supercond. **3**, 2337-40 (1993)

[7] J. Du, J.C. Macfarlane, T. Zhang, Y. Cai and Y.J. Guo, Self-pumped HTS Josephson heterodyne tunable mixer, Supercond. Sci. Technol. **25**, 025019 (2012)

[8] J. Du and J.C. Macfarlane, Frequency down-conversion in self-pumped HTS R-SQUID mixer, Electron. Lett. **47**, 772 (2011)

[9] I.K. Yanson, V.M. Svistunov, I.M. Dmitrenko, Experimental observation of tunnel effect for cooper pairs with emission of photons, JETP **21**, 650 (1965)

[10] E. Stepantsov, M. Tarasov, A. Kalabukhov, L. Kuzmin, and T. Claeson, THz Josephson properties of grain boundary YBaCuO junctions on symmetric, tilted bicrystal sapphire substrates, J. Appl. Phys. **96**, 15 (2004)

[11] I. E. Batov, X.Y. Jin, S.V. Shitov, Y. Koval, P. Mller, and A.V. Ustinov, Detection of 0.5 THz radiation from intrinsic $Bi_2Sr_2CaCu_2O_8$ Josephson junctions, Appl. Phys. Lett. **88**, 262504 (2006)

[12] M. Tarasov, E. Stepantsov, T. Lindstrom, A. Lohmus, L. Kuzmin, and Z. Ivanov, Submillimeter-wave quasioptical integrated tester based on bicrystal Josephson junctions, Physica C **372-376**, 347 (2002)

[13] L. Ozyuzer, A.E. Koshelev, C. Kurter, N. Gopalsami, Q. Li, M. Tachiki, K. Kadowaki, T. Yamamoto, H. Minami, H. Yamaguchi, T. Tachiki, K.E. Gray, W.-K. Kwok, and U. Welp, Emission of coherent THz radiation from superconductors, Science **318**, 1291 (2007)

[14] I. Kakeya, Y. Omukai, T. Yamamoto, K. Kadowaki, and M. Suzuki, Effect of thermal inhomogeneity for terahertz radiation from intrinsic Josephson junction stacks of $Bi_2Sr_2CaCu_2O_{8+\delta}$, Appl. Phys. Lett. **100**, 242603 (2012)

[15] D.Y. An, J. Yuan, N. Kinev, M.Y. Li, Y. Huang, M. Ji, H. Zhang, Z.L. Sun, L. Kang, B.B. Jin, J. Chen, J. Li, B. Gross, A. Ishii, K. Hirata, T. Hatano, V.P. Koshelets, D. Koelle, R. Kleiner, H.B. Wang, W.W. Xu, and P.H. Wu, Terahertz emission and detection both based on high-Tc superconductors: Towards an integrated receiver, Appl. Phys. Lett.**102**, 092601 (2013)

[16] O. Astafiev, S. Komiyama, Single-photon detection with quantum dots in the far-infrared/submillimeter-wave range, *Electron Transport in Quantum Dots*, ed. J Bird, Dordrecht, Kluwer (2003)

[17] E. Stepantsov, M. Tarasov, A. Kalabukhov, T. Lindstrom, Z. Ivanov, T. Claeson, Submicron YBCO Josephson junctions on sapphire bicrystal substrates for microwave devices, Physica C **372-376**, 76 (2002)

[18] M. Tihkham, M. Octavio, W. Scocpol, Heating effects in high?frequency metallic Josephson devices: Voltage limit, bolometric mixing, and noise, J.Appl.Phys. **48**, 1311 (1977)

[19] O. Astafiev, S. Komiyama, T. Kutsuwa, V. Antonov, Y. Kawaguchi, K. Hirakawa, Single-photon detector in the microwave range, Appl. Phys. Lett. **80**, 4250 (2002)

[20] O. Astafiev, V. Antonov, T. Kutsuwa, S. Komiyama, Far-infrared spectroscopy of single quantum dots in high magnetic fields, Phys. Rev. B **65**, 085315 (2002)

[21] V.M. Muravev, and I.V. Kukushkin, Plasmonic detector/spectrometer of subterahertz radiation based on two-dimensional electron system with embedded defect, Appl. Phys. Lett. **100**, 082102 (2012)

[22] F. Teppe, W. Knapp, D. Veksler, M.S. Shur, A.P. Dmitriev, V.Yu. Kachorovskii, and S. Rumyantsev, Room-temperature plasma waves resonant detection of sub-terahertz radiation by nanometer field-effect transistor, Appl. Phys. Lett. **87**, 052107 (2005)

[23] J.W. Song, N.A. Kabir, Y. Kawano, K. Ishibashi, G.R. Aizin, L. Mourokh, J.L. Reno, A.G. Markelz, and J.P. Bird, Terahertz response of quantum point contacts, App. Phys. Lett. **92**, 223115 (2008)

[24] S. Pelling, E. Otto, S Spasov, S. Kubatkin, R. Shaikhaidarov, K. Ueda, S. Komiyama and V.N Antonov, Electrostatic effects in coupled quantum dot-point contact-single electron transistor devices, J. Appl. Phys **112**, 014322 (2012)

[25] M. H. Devoret, and R. J. Schoelkopf, Amplifying quantum signals with the single-electron transistor, Nature **406**, 1039 (2000)

[26] J. Edstam, G. Brorsson, E.A. Stepantsov and H.K. Olsson, Integrated High-T_c oscillator array and high resistance detector junction, IEEE Trans. Appl. Supercond. **5**, 3276 (1995)

[27] J. Edstam, P. Larsson, E.A. Stepantsov and H.K. Olsson, Phase locking of an array of five High-T_c Josephson junction oscillators, Physica C **235-240**, 3385 (1994)

[28] M. Darula, T. Doderer and S. Beuven, Millimetre and sub-mm wavelength radiation sources based on discrete Josephson junction arrays, Supercond. Sci. Technol. **12**, R1 (1999)